Semiconductor Physics, Quantum Electronics & Optoelectronics, 2022. V. 25, No 3. P. 254-261.

Semiconductor physics

Spin-dependent polarization response in HgCdTe hot-electron bolometers

F.F. Sizov[1*], J.V. Gumenjuk-Sichevska[1], S.N. Danilov[2], Z.F. Tsybrii[1]

[1]V. Lashkaryov Institute of Semiconductor Physics, NAS of Ukraine,
41, prosp. Nauky, 03680 Kyiv, Ukraine
[2]Terahertz Center, University of Regensburg, 93040 Regensburg, Germany
**Corresponding author e-mail: sizov@isp.kiev.ua*

Abstract. The paper reports the detection of strong polarization-dependent photo-responses in direct narrow-gap (E_g = 0.084 eV at T = 80 K) HgCdTe thin-layer biased and unbiased hot-electron bolometers (HEBs) with receiving antennas under elliptically polarized THz radiation. The observed effects are assumed to be due to the Rashba spin splitting in HgCdTe, caused by large spin-orbit interactions. The studied detectors demonstrate free-carrier polarization-dependent sensitivity to laser radiation with $h\nu \approx 0.0044$ eV (ν = 1.07 THz) and 0.0025 eV (ν = 0.6 THz), *i.e.*, with photon energies much less than the band-gap ($h\nu << E_g$) at T = 80 and 300 K. The polarization-dependent photocurrent in HgCdTe HEBs with and without applied external constant electric field is shown to have angular dependence of photocurrent with directional reversal on switching the photon helicity.

Keywords: THz antenna-coupled hot-electron bolometer, THz elliptically polarized radiation, polarization-dependent photo-response, narrow-gap HgCdTe.

https://doi.org/10.15407/spqeo25.03.254
PACS 73.50.Pz, 73.61.Ga, 85.75.-d

Manuscript received 19.05.22; revised version received 18.08.22; accepted for publication 21.09.22; published online 06.10.22.

1. Introduction

Spin-oriented effects attract attention for rather long time. The Rashba effect (*i.e.*, spin degeneracy lifting by built-in constant electric field in solid state crystals, in particular, heterostructures) caused by the strong spin-orbit interaction (SOI) was discovered in 1959. Originally, it was proposed for non-centrosymmetrical wurtzite semiconductors, in which lack of inversion centers results in the spin-orbit splitting of electron energy bands [1]. As was pointed out in [2], the Rashba spin-orbit coupling inspired a large number of predictions, discoveries and innovative concepts during the past 30 years not only in the field of semiconductors. During the last decade, the realizations of manipulating spin orientation was demonstrated thought the spin Hall effect, spin-orbit qubits, topological insulators, cold-atom systems, Dirac materials, *etc*. [2, 3].

The Rashba effect has enabled to control conduction electron spins in microelectronic devices conditioned with the spin-dependent phenomena in condensed matter. These phenomena occur due to spin-orbit interaction (SOI), which is a relativistic effect, when electron spin is propagating in the mean electric field of solid-state crystals and structures that corresponds to periodic crystal potential or an external one. SOI is the basis of semiconductor spintronics. It provides a mechanism of the generation and manipulation of spins by electric fields. In III-V or II-VI (here HgCdTe – mercury-cadmium-telluride – MCT) narrow-gap semiconductors with zinc-blende structure, SOI in the conduction band (c-band) occurs due to **k-p**-mixing with other bands, mainly with the valence one (v-band). Taking into account only Γ_6, Γ_8 and Γ_7 bands in the eight-band Kane model, non-centrosymmetric crystals are not considered.

Because of the free-carrier sensitivity of HgCdTe detectors in the THz range [4] one aims to study the influence of polarized THz radiation on the angular dependence of free-carrier photo-response due to possible Rashba spin splitting in the conduction band.

Spin-dependent electrical currents are usually generated by electrical or magnetic fields, by gradients of carrier concentration or by temperature when certain symmetry requirements are fulfilled. The electric control of spin states is superior to magnetic field control due to its better scalability, lower power consumption and the possibility of the local manipulation of spin states [2]. The Rashba effect is a momentum-dependent spin-orbit splitting of electron states in bulk uniaxial non-centrosymmetric crystals (*e.g.*, wurtzite or zinc blende ones, where it occurs due to the presence of macroscopic

internal or external electric fields as well as mechanical stresses) and low-dimensional systems (*e.g.*, quantum wells, QWs). This spin-oriented effect can be the reason for a number of spin-dependent phenomena in semiconductors.

In a two-dimensional spectrum in asymmetrical quantum well when, because of reduced symmetry in some crystallographic directions, this spin splitting can appear. In two-dimensional quantum wells with similar heterostructure barriers, the potential is symmetrical and Rashba spin splitting leading to spin-dependent current caused by macroscopic electric field is equal to zero. If an external electric field is applied to one of the planes of QW or the potentials at both planes of heterostructure are not equal (an asymmetric potential), a momentum-dependent splitting of spin bands takes place [5] (the Rashba effect, sometimes also called the Bychkov–Rashba effect). Such phenomenon can be also observed in bulk crystals with certain symmetry under the external electric field or mechanical stress. External electric field or stress lowers the symmetry of the "crystal + field" system. Spin splitting in the spectrum of 2D electrons was also considered in [6, 7].

In the phenomenological Rashba model of two-dimensional energy spectrum (parabolic model), an additional term proportional to the wave vector k with the Rashba parameter α_R as proportionality factor is added to $\hbar^2 \cdot k^2/2m^*$:

$$E\pm = \hbar^2 k^2 / 2m^* \pm \alpha_R \cdot k , \qquad (1)$$

where m^* is the effective electron mass, k is the wave vector, and the term $\alpha_R \cdot k$ appears due to the account of SOI.

The additional term in the Hamiltonian of electron in the conduction band of an asymmetric quantum well with low crystal symmetry resulted from SOI has the following form [5]:

$$H_{so} = \alpha_R \cdot [\boldsymbol{\sigma} \times \mathbf{k}] \cdot \boldsymbol{\nu} , \qquad (2)$$

where $\boldsymbol{\sigma}$ are the Pauli matrices and $\boldsymbol{\nu}$ is the unit vector, respectively. H_{so} lifts the two-fold spin degeneracy at $\mathbf{k} \neq 0$ and determines the spin-orbit splitting near $\mathbf{k} = 0$. In semiconductors with non-parabolic dispersion law (*e.g.*, InSb or HgCdTe), the physical meaning of Rashba splitting does not change. It was shown in [8] that strain also induces appearance of an additional SOI-related term for bulk zinc blende crystals.

Earlier results of Rashba splitting refer to 2D semiconductor systems. In bulk semiconductors (3D systems), the Rashba contribution to the Hamiltonian (2) can be obtained considering 3D semiconductor in an external electric field. External electric field lowers the symmetry of such system lifting the center of spatial inversion and the Hamiltonian (2) acquires the similar form with $\boldsymbol{\nu} = \mathbf{E}/|E|$ [9].

Presence of external electric field can lift the spin degeneracy in non-centrosymmetric media (*e.g.*, narrow-gap HgCdTe semiconductors and semiconductor heterostructures with zinc-blende structure belonging to the space group $\bar{4}3m\left(T_d^2\right)$, point group $\bar{4}3m\left(T_d\right)$) [9]. This is demonstrated in the framework of the Kane band model taking into account only the conduction band Γ_6 and the valence band Γ_8. Therefore, optical polarization-oriented response in the THz range can be obtained even in zero magnetic field. In zero-biased semiconductors and heterostructures, the driving electric field of the intence THz electromagnetic wave can induce nonequilibrium spin polarization of electrons and generation of charge current observed in unbiased HgCdTe objects (see, *e.g.*, [10, 11]).

Two types of spin splitting at zero magnetic field arising due to the structure and bulk inversion asymmetry are mainly found in semiconductors [12, 13], namely the Rashba and the Dresselhaus ones [14, 15].

The Rashba spin splitting generally occurs due to the spatial inhomogeneity at the interface or surface [15, 16]. It is dominant in narrow-gap semiconductors [17]. The Rashba effect can be controlled by external electric fields and strain and attracts an especial attention due to its tunability by the former.

Here, some results, in honor of Prof. E.I. Rashba, who worked for a long time at the Institute of Physics and the V. Lashkaryov Institute of Semiconductor Physics of the National Academy of Sciences of Ukraine, are presented. These results concern spintronic phenomena in narrow-gap HgCdTe thin films in external constant electric field and without it and are considered, to some degree, according to research performed in [18].

2. Considerations and estimations

Bulk semiconductors with a zinc blende lattice (such as HgCdTe crystals and epitaxial layers) are non-gyrotropic. Such influences as strain or external constant electric field, which reduce the crystal symmetry, with or without applied bias, can lead to current-induced spin polarization (CISP) response due to the spin splitting effect and be a reason of polarization-dependent photo-response observed in HgCdTe free-carrier bolometers.

Since the intrinsic spin-orbit interaction in narrow-gap HgCdTe or InSb is strong, spin splitting (the Rashba effect) in an electric field should be more pronounced as compared to other semiconductors at the same field strength (see, *e.g.*, [17]). Although the Rashba spin splitting in semiconductors is relatively small, it may be still important for the explanation of photo-response in "thick" ($d \approx 2.4$ μm) relatively long (10–18 μm, to sum up the spin-influenced effects) antenna-coupled biased narrow-gap HgCdTe photoconductors. Such photoconductors are perspective for the development of polarization-sensitive fast detectors, which is important, *e.g.*, for recording full THz radiation polarization state [19, 20].

Among the known semiconductors, $Hg_{1-x}Cd_xTe$ narrow-gap semiconductors with $x \approx 0.10…0.25$ have the largest value of SOI. The conduction electron states are strongly mixed with the valence states through the $\mathbf{k}\cdot\mathbf{p}$-interaction across a narrow energy gap. This interaction is strong in narrow-gap semiconductors, leading to large values of electron g-factor [21, 22].

Here, the polarization-dependent photo-response is considered for inter-sub-band absorption of circularly and linearly polarized THz radiation in HgCdTe HEBs. This process is presumably considered to be a spin-dependent one. It was shown in [18] that the magnitude and sign of photo-response depend on the degree of polarization related to the difference of the rates of spin transitions parallel and antiparallel to light polarization. This is the base for a spin-galvanic effect (SGE), *i.e.*, electric current flow induced by asymmetrical spin relaxation.

The Rashba Hamiltonian for spin-orbit interaction in non-parabolic bulk semiconductors (*i.e.*, when the Kane model is applicable) in an external static electric field, which withdraws the center of crystal spatial inversion, has formally a similar form to Eq. (2) [9]:

$$H_{eff} = \xi_{so} \cdot q \cdot [\boldsymbol{\sigma} \times \mathbf{k}] \cdot \mathbf{E}, \quad (3)$$

where q is the electron charge and E is the electric field strength, respectively.

The material-specific coefficient ξ_{so} is the spin-orbit coupling parameter (the Rashba spin splitting energy for electrons in the *c*-band). It depends on the momentum matrix element, the energy of spin-orbit splitting and the band-gap [9, 23]:

$$\xi_{so} = -\frac{P_0^2}{3} \times \frac{\Delta_0 \cdot (2E_g + \Delta_0)}{E_g^2 (E_g + \Delta_0)^2}. \quad (4)$$

Here, P_0 is the inter-band momentum matrix element, E_q is the band-gap (the separation between the Γ_6-conduction band and Γ_8-valence band edges), and Δ_0 is the energy of spin-orbit splitting (the separation between the Γ_8-valence band and Γ_7-valence band edges), respectively.

For GaAs with small spin-orbit splitting, the estimations result is $\xi_{so} \approx 5 \cdot 10^{-20}$ m^2. ξ_{so} (InSb, E_q(80 K) = 0.23 eV, $\Delta_0 \approx 0.9$ eV) $\approx 5.5 \cdot 10^{-18}$ m^2. For *n*-$Hg_{0.799}Cd_{0.201}Te$ (E_q(80 K) $\approx$ 0.084 eV, $\Delta_0 \approx 0.98$ eV) studied here, the value $\xi_{so} \approx 3.3 \cdot 10^{-17}$ m^2 (P_0(HgCdTe) = $8.3 \cdot 10^{-8}$ eV·cm). Therefore, the influence of constant electric field on the current-induced spin should be pronounced in *n*-type $Hg_{0.799}Cd_{0.201}Te$ semiconductor even at weak electric fields. However, influence of mechanical strain caused by the mismatch of the lattice constants of GaAs substrate and HgCdTe (Δa_0 = 13.6%) even with buffer layers between them on SOI leading to the appearance of spin-dependent effects cannot be also excluded. To reduce the lattice mismatch, photosensitive HgCdTe layers were grown on (013)-oriented GaAs substrates with ZnTe (0.01 μm) and CdTe (5…7 μm) buffer layers (Fig. 1).

To fabricate THz $Hg_{1-x}Cd_xTe$ ($x \approx 0.201$) thin HEBs (the thickness $d \approx 2.4$ μm), the layers were grown by molecular beam epitaxy (MBE).

The estimated values $\xi_{so} \cdot q \cdot E \approx (1.42…2) \cdot 10^{-13}$ eV·m in $Hg_{0.799}Cd_{0.201}Te$ were obtained at the typical low electric field strengths of $(4.5…7) \cdot 10^3$ V/m. Such electric fields were used in the experiments described below.

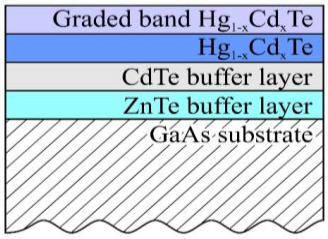

Fig. 1. Schematic image of the layered structure of HgCdTe HEB.

The values of $\xi_{so} \cdot q \cdot E$ are smaller than the typical Rashba spin splitting parameters $\alpha_R = 8.1 \cdot 10^{-12}$ eV·m and α_R = $(4…7) \cdot 10^{-12}$ eV·m for AlGaN/GaN and InGaAs/InAlAs 2D heterostructures, respectively [24, 25]. In spite of the relatively small values of $\xi_{so} \cdot q \cdot E$ coefficient, the influence of spin-orbit effects on the sensitivity of relatively thin ($d \approx 2.4$ μm) narrow-gap photoconductors under powerful THz radiation could be observed. But even without bias a smaller by an order of magnitude polarization photo-response was detected under the elliptically polarized THz radiation, which was apparently due to residual mechanical stresses in HgCdTe layers (see below).

3. Experimental

The $Hg_{1-x}Cd_xTe$ MBE epitaxial layers [26] (band-gap $E_g \approx 0.084$ eV at T = 80 K) had *n*-type conductivity and the measured values of the carrier concentration $N \approx 1.4 \cdot 10^{14}$ cm^{-3} and the mobility $\mu \approx 96000$ cm^2·V^{-1}·s^{-1} at $T \approx 80$ K. The deviations of GaAs surface from the (013) orientation were 1°…3°, while for ZnTe/CdTe buffer layers they amounted up to 8° [27]. The antenna blades were formed by two-layer metal contacts [28] (Mo + Au(In)) to bias MCT photoconductors. The photo-response was studied at 280 μm ($h\nu \approx 0.0044$ eV) and 496 μm ($h\nu$ = 0.0025 eV) under normally incident radiation to (013)-oriented films. To study the response of MCT HEBs to various polarization states of radiation, a linearly polarized laser beam was transmitted through λ/4 or λ/2-plates made of *x*-cut crystalline quartz (see Figs 2 and 3).

We studied the polarization-dependent detector response under the THz radiation from a pulsed gas laser with CO_2 laser pumping. The laser generation energies at the wavelengths 280 μm (ν = 1.07 THz, $h\nu \approx 0.0044$ eV) and 495 μm (ν = 0.6 THz, $h\nu \approx 0.0025$ eV) were much less than the band-gap of $Hg_{0.201}Cd_{0.799}Te$ (0.084 eV at T = 80 K). Therefore, the THz radiation was absorbed by free carriers (electrons), which led to their heating. The diameter of radiation spot was about 1.5…2.5 mm depending on the laser emission wavelength. The radiation pulse length varied from 75 to 100 ns for different THz frequencies. The peak intensity of THz laser power was controlled by a fast room-temperature pyroelectric detector and reached about $P \approx$ 10 kW/3.5 kW for the radiation frequencies ν = 0.6 THz and 1.07 THz, respectively. The laser beams had nearly Gaussian shapes and

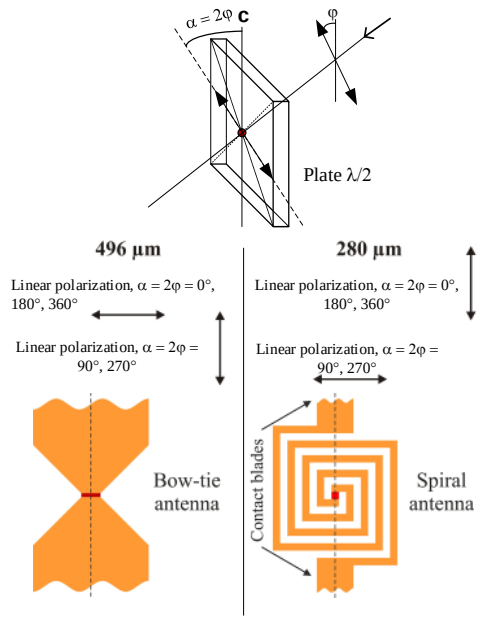

Fig. 2. Positions of the axes of antennas relative to the polarization states of linearly polarized laser radiation with the wavelengths of 496 and 280 μm. Polarization state is defined by the angle α = 2φ, where φ is the angle between the optical axis of a λ/2 (λ/4) plate and the initial linear (plane) polarization direction (initial plane of linear polarization). The areas of the sensitive parts of HEBs did not exceed ~500 μm^2. The areas of the detectors with antennas were comparable to the wavelengths of radiation.

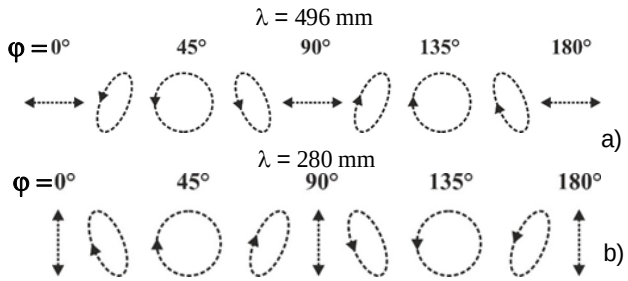

Fig. 3. Linearly, elliptically, and circularly polarized states of laser radiation with the wavelengths of 496 (*a*) and 280 μm (*b*), respectively, which passed through the λ/4 plate. φ is the angle between the initial plane of linear polarization and the optical axis of λ/4 plate.

were focused onto HEBs by a parabolic mirror. The lock-in amplifier was loaded with low-resistance cables (~50 Ohm). The measurements were performed in the photocurrent generation mode.

Rotation of λ/4 plate by the angle φ with respect to the initial laser polarization plane resulted in the variation of radiation polarization state. The degree of circular polarization P_{circ} of elliptically polarized radiation after passing through the λ/4 plate changed as follows [29]:

$$P_{circ} = \frac{I^{\sigma^+} - I^{\sigma^-}}{I^{\sigma^+} + I^{\sigma^-}} = \sin(2\varphi). \qquad (5)$$

Biased and unbiased HgCdTe HEBs demonstrate appearance of an additional angular-dependent current to the ordinary charge current (see Figs 4 and 5). The data and fitting curves are symmetrical at biases of different signs. To save the space, the fitting parameters for only some exemplary experimental data are presented here. The observed photo-response results are similar for spiral and bow-tie antennas.

The response of unbiased structure without rectifying contacts at T = 300 K is small and almost does not depend on polarization angle. However, pronounced signals are observed at lower temperature T = 80 K at zero bias (see Fig. 5). These signals are still more than an order of magnitude smaller as compared to the ones at current biases of +/–250 μA. The angular dependences of such small signals can be the reason for appearance of mechanical strain in HgCdTe layers on GaAs substrates [29].

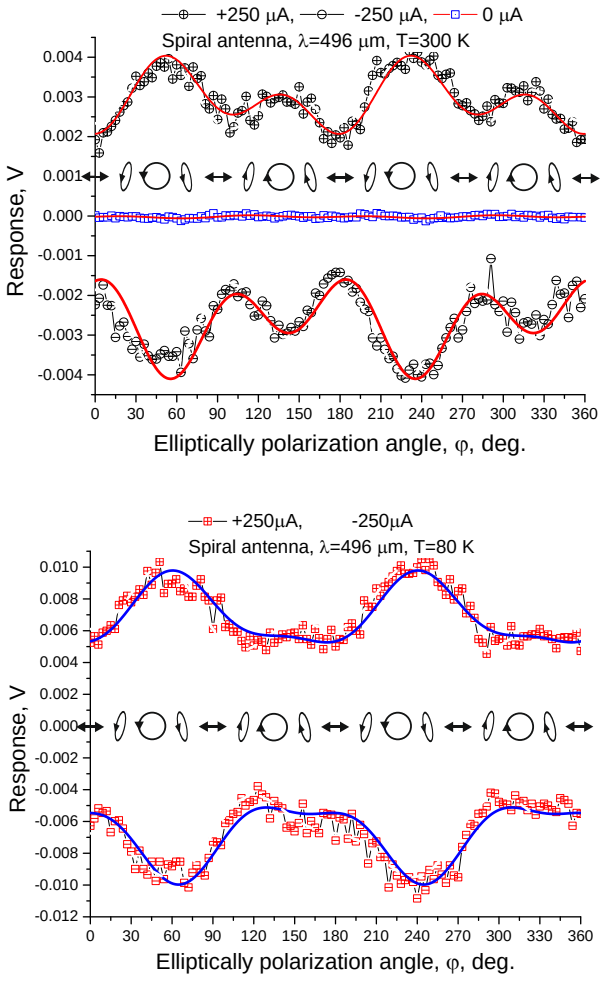

Fig. 4. Photo-response of MCT HEB with spiral antenna as a function of laser radiation helicity (λ = 496 μm) measured at room (*a*) and liquid nitrogen (*b*) temperatures. The laser elliptical polarization conditions are sketched according to the phase angle φ. Measurements (symbols) were carried out at different biases. Solid lines show the fitting curves constructed by Eq. (6) with $\varphi_0 = 18°$.

To build up the fitting curves, the overall polarization dependence [29] was used:

$$U_{response} = U_0 + U_c \sin\left[2(\varphi-\varphi_0)\right] + \\ + U_{L1}\frac{\cos\left[4(\varphi-\varphi_0)\right]+1}{2} + U_{L2}\frac{\sin\left[4(\varphi-\varphi_0)\right]}{2}. \quad (6)$$

It describes well the circular photo-galvanic effect (CPGE), causing induction of a photocurrent. The direction of this photocurrent is reversed upon switching the photon helicity at zero bias (Figs 4 and 5). The sign of response is reversed when the bias current changes from "+" to "–" (Fig. 4).

In Eq. (6), U_i are the fitting parameters (the linear polarized signal is fitted using the amplitudes U_{L1} and U_{L2}, and circular polarized signal amplitude is fitted using the coefficient U_c) and

$$P_{L1} = \frac{\cos(4\varphi)+1}{2}, \quad P_{L2} = \frac{\sin(4\varphi)}{2} \quad (7)$$

are the Stokes parameters defining the degree of the linear polarization of elliptically polarized radiation, respectively. To achieve better fitting, the polarization angle in Figs 4 and 5 is shifted by φ_0 = 18°, which is presumably related to the miss-orientation of sample crystallographic axes [18] toward the ones shown in Fig. 3. The total photocurrent also contains a polarization-independent shift U_0, an amplitude coefficient of photo-response to elliptical polarization U_c (2φ-dependence), the angular dependence of which has a period of π, and a photo-response to linear polarization (with the amplitudes U_{L1} and U_{L2}) having a period of π/2 (4φ-dependences). The solid curves were obtained by the fitting procedure discussed in detail, *e.g.* in [18, 29, 30].

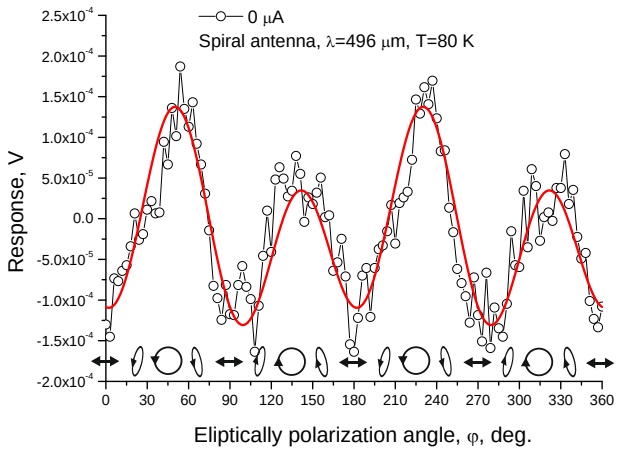

Fig. 5. Photo-response of HgCdTe HEB with spiral antenna as a function of laser radiation helicity (λ = 496 μm) measured at T = 80 K. The laser elliptically polarization conditions are sketched according to the phase angle φ. Symbols are the experimental data and the solid line is fitted by Eq. (6). The polarization angle is shifted by φ_0 = 18°. $U_0 = 5.171\cdot10^{-5}$, $U_c = 2.617\cdot10^{-5}$, $U_{L1} = -1.340\cdot10^{-4}$, and $U_{L2} = 1.516\cdot10^{-4}$.

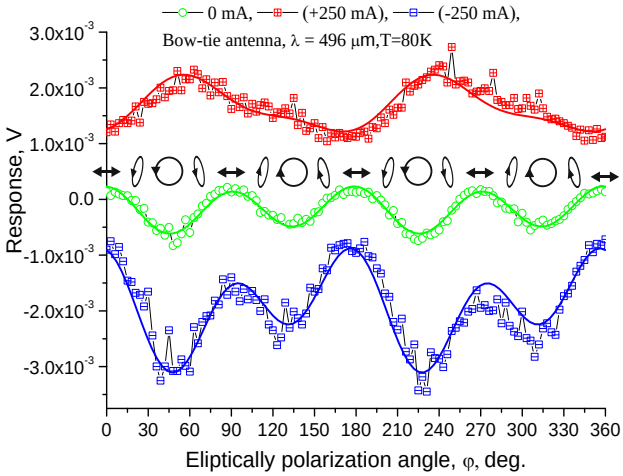

Fig. 6. Photo-response of MCT HEB with bow-tie antenna as a function of laser radiation helicity (λ = 496 μm) measured at T = 80 K. The laser circular polarization conditions are sketched according to the phase angle φ. Measurements (symbols) were carried out at different biases. Solid lines are fitted by Eq. (6) with φ_0 = 18°.

As can be seen from Fig. 6, for detectors with rectifying contacts the photo-response dependences are asymmetrical at I_{bias} = +/–250 μA because of the shifted dependence at I_{bias} = 0. The shift of the latter one is presumably caused by the presence of the built-in electrical field of rectifying contact (Schottky barrier) at antenna blades. Moreover, since the direction of built-in electric field due to the rectifying contact coincides with the one of applied electric field, the curve at zero bias for the sample with ohmic contacts (see Fig. 5) is opposite in direction reverses upon switching the photon helicity at I_{bias} = 0 for the samples with rectifying contacts.

The polarization-dependent photo-responces at ν = 1.07 THz are weaker as compared to those at ν = 0.6 THz. Their character is, however, the same, hence, they are not shown here. The response signals follow the temporal structure of a laser pulse. The decay time of THz signal is of the order of pulse relaxation time τ ~ 75 ns. The distances between the antennas edges were from 10 to 18 μm.

4. Conclusions

The polarization-dependent free-carrier photo-responses in narrow-gap HgCdTe thin-layer HEBs with large spin-orbit coupling inherent to this material was observed and studied at the THz frequencies ν = 1.07 THz ($h\nu \approx$ 0.0044 eV) and 0.6 THz ($h\nu \approx$ 0.0025 eV), and T = 80 and 300 K. Two types of antennas (bow-tie and spiral ones) were formed to input the radiation into small sensitive areas (≤ 500 μm^2) of HEBs. The photon energies of THz radiation were much smaller than the band-gap E_g of $Hg_{0.201}Cd_{0.799}Te$ (E_g = 0.084 eV at T = 80 K).

The angular dependences of photocurrent demonstrate the directional reversal on switching the photon helicity. More than one order of magnitude weaker polarization-dependent photocurrents in HgCdTe HEBS with antennas are observed at 80 K at $E = 0$. The free-carrier polarization-dependent photocurrent at $E = 0$ in the samples with ohmic contacts is caused by the spin splitting Rashba-type phenomena, which take place due to the structure-induced asymmetry caused by the residual strain in HgCdTe layers on GaAs substrates. The detectors under study are based on the bulk epitaxially grown $Hg_{1-x}Cd_xTe$ ($x = 0.201$) films with normal band order structure ($E_g > 0$) in the crystallographic plane (013). ZnTe and CdTe buffer layers were used to reduce mechanical stresses in HgCdTe layers caused by the mismatch of lattice constants between the GaAs substrates and HgCdTe.

Acknowledgements

We are grateful to Professor S. Ganichev for providing opportunities to carry out experiments as well as for fruitful discussions.

This work was partly supported by the Volkswagen Foundation Partnerships-Cooperation Project "Terahertz optoelectronics in novel low-dimensional narrow-gap semiconductor nanostructures" (project number 97738) and the NAS of Ukraine, project No. III-3-22. S.N. Danilov gratefully acknowledges the support of the Deutsche Forschungsgemeinschaft (DFG) (Project-ID 314695032 – SFB 1277) and the Elite 253 Network of Bavaria (K-NW – 2013-247).

References

1. Rashba E.I. and Sheka V.I. Symmetry of energy bands in crystals of wurtzite type. *Fizika Tverd. Tela* – Collected Papers (Leningrad). 1959. II. P. 162–176 (in Russian).
2. Manchon A., Koo H.C., Nitta J., Frolov S.M. and Duine R.A. New perspectives for Rashba spin-orbit coupling. *Nature Materials.* 2015. **14**. P. 871–882. https://doi.org/10.1038/nmat4360.
3. Bihlmayer G., Rader O. and Winkler R. Focus on the Rashba effect. *New J. Phys*. 2015. **17**. P. 050202. http://dx.doi.org/10.1088/1367-2630/17/5/050202.
4. Sizov F., Zabudsky V., Dvoretskii S. *et al*. Two-color detector: Mercury-cadmium-telluride as a terahertz and infrared detector. *Appl. Phys. Lett*. 2015. **106**. P. 082104. https://doi.org/10.1063/1.4913590.
5. Bychkov Yu.A., Rashba E.I. Properties of a 2D electron gas with lifted spectral degeneracy. *JETP Lett*. 1984. **39**, issue 2. P. 78–81.
6. Vas'ko F.T., Prima N.A. Spin splitting of the spectrum of two-dimensional electrons. *Solid State Phys*. 1979. **21**. P. 1734–1738 (in Russian).
7. Vas'ko F.T. Spin splitting in the spectrum of two-dimensional electrons due to the surface potential. *JETP Lett*. 1979. **30**. P. 541–544.
8. Dyakonov M.I. and Kachorovskii V.Y. Spin relaxation of two dimensional electrons in noncentrosymetric semiconductors. Soviet Physics: *Semiconductors*. 1986. **20**. P. 110–116.
9. Glazov M.M. *Spin Phenomena in Semiconductors*. Lecture Course, 2018 (in Russian).
10. Ganichev S.D., Ivchenko E.L., Bel'kov V.V. *et al*. Spin-galvanic effect. *Nature.* 2002. **417**. P. 153–156. https://doi.org/10.1038/417153a.
11. Danilov S.N., Wittmann B., Olbrich P. *et al*. Fast detector of the ellipticity of infrared and terahertz radiation based on HgTe quantum well structures. *J. Appl. Phys.* 2009. **105**. P. 013106. https://doi.org/10.1063/1.3056393.
12. Bychkov Y.A., Rashba E.I. Oscillatory effects and the magnetic susceptibility of carriers in inversion layers. *J. Phys. C: Solid State Phys*. 1984. **17**. P. 6039. https://doi.org/10.1088/0022-3719/17/33/015.
13. Dresselhaus G. Spin-orbit coupling effects in zinc blende structures. *Phys. Rev. B*. 1955. **100**. P. 580–586. https://doi.org/10.1103/PhysRev.100.580.
14. Ivchenko E.L. and Ganichev S.D. Spin Photogalvanics. M.I. Dyakonov (Ed.). *Spin Physics in Semiconductors*. Berlin, Springer, 2017. https://doi.org/10.1007/978-3-319-65436-2.
15. Ganichev S.D., Golub L.E. Interplay of Rashba/Dresselhaus spin splittings probed by photogalvanic spectroscopy – A review. *phys. status solidi* (*b*). 2014. **251**. P. 1801–1823. https://doi.org/10.1002/pssb.201350261.
16. Stein D., Klitzing K., Weimann G. Electron spin resonance on GaAs–$Al_xGa_{1-x}As$ heterostructures. *Phys. Rev. Lett*. 1983. **51**. P. 130–133. https://doi.org/10.1103/PhysRevLett.51.130.
17. Lommer G., Malcher F., Rossler U. Spin splitting in semiconductor heterostructures for B→0. *Phys. Rev. Lett.* 1988. **60**. P. 728–731. https://doi.org/10.1103/PhysRevLett.60.728.
18. Sizov F., Tsybrii Z., Danilov S. *et al*. THz polarization-dependent response of antenna-coupled HgCdTe photoconductors under an external constant electric field. *Semicond. Sci. Technol*. 2021. **36**. P. 105009. https://doi.org/10.1088/1361-6641/ac1770.
19. Olbrich P., Zoth C., Vierling P. *et al*. Giant photocurrents in a Dirac fermion system at cyclotron resonance. *Phys. Rev. B*. 2013. **87**. P. 235439. https://doi.org/10.1103/PhysRevB.87.235439.
20. Peng K., Jevtics D., Zhang F. *et al*. Three-dimensional cross-nanowire networks recover full terahertz state. *Science*. 2020. **368**. P. 510–513. https://doi.org/10.1126/science.abb0924.
21. Litvinenko K.L., Nikzad L., Pidgeon C.R. *et al*. Temperature dependence of the electron Landé g factor in InSb and GaAs. *Phys. Rev. B*. 2008. **77**. P. 033204. https://doi.org/10.1103/PhysRevB.77.033204.
22. Kim R.S., Narita S. Far-infrared interband magneto-absorption and band structure of $Hg_{1-x}Cd_xTe$ alloys. *phys. status solidi* (*b*). 1976. **73**. P. 741. https://doi.org/10.1002/pssb.2220730244.

23. Radantsev V.F., Yafyasov A.M. Rashba splitting in MIS structures HgCdTe. *J. Exp. Theor. Phys*. 2002. **95**. P. 491–501. https://doi.org/10.1134/1.1513822.
24. Morrison C., Wiśniewski P., Rhead S.D. *et al*. Observation of Rashba zero-field spin splitting in a strained germanium 2D hole gas. *Appl. Phys. Lett*. 2014. **105**. P. 182401. https://doi.org/10.1063/1.4901107.
25. Yao Q., Cai J., Tong W. *et al*. Manipulation of the large Rashba spin splitting in polar two-dimensional transition-metal dichalcogenides. *Phys. Rev. B.* 2017. **95**. 165401. https://doi.org/10.1103/PhysRevB.95.165401.
26. Dvoretsky S.A., Mikhailov N.N., Remesnik V.G. *et al*. *Opto-Electron. Rev.* 2019. **27**. P. 282. https://doi.org/10.1016/j.opelre.2019.07.002.
27. Stupak M.F., Mikhailov N.N., Dvoretskii S.A. *et al*. Possibilities of characterizing the crystal parameters of $Cd_xHg_{1-x}Te$ structures on GaAs substrates by the method of generation of the probe-radiation second harmonic in reflection geometry. *Phys. Solid State.* 2020. **62**. P. 252–259. https://doi.org/10.1134/S1063783420020201.
28. Sizov F., Tsybrii Z., Apats'ka M. *et al*. Ohmic metal/$Hg_{1-x}Cd_xTe$ ($x \approx 0.3$) contacts. *Semicond. Sci. Technol*. 2020. **35**. P. 125030. https://doi.org/10.1088/1361-6641/abc0f7.
29. Hubmann S., Budkin G.V., Otteneder M. *et al*. Symmetry breaking and circular photogalvanic effect in epitaxial $Cd_xHg_{1-x}Te$ films. *Phys. Rev. Materials.* 2020. **4**. P. 043607. https://doi.org/10.1103/PhysRevMaterials.4.043607.
30. Tsybrii Z., Danilov S., Gumenjuk-Sichevska J., Mikhailov N., Dvoretskii S., Melezhik E., Sizov F. Spintronics phenomena induced by THz radiation in narrow-gap HgCdTe thin films in an external constant electric field. *Semiconductor Physics, Quantum Electronics & Optoelectronics*. 2021. **24**. P. 185–191. https://doi.org/10.15407/spqeo24.02.185.

Authors' contributions

Fedir Sizov: conceptualization, methodology, formal analysis, resources, writing – original draft, writing – review & editing.

Joanna Gumenjuk-Sichevska: conceptualization, methodology, validation, formal analysis, investigation, resources, data curation, writing – vizualization, review & editing.

Sergey Danilov: experimental methodology, data curation (partially), validation.

ZinoviiaTsybrii: investigation, data curation (partially), review & editing.

Authors and CV

Fedir Sizov, Doctor of Sciences in Physics and Mathematics, Professor, Corresponding Member of NAS of Ukraine, Head of Department at the V. Lashkaryov Institute of Semiconductor Physics, NAS of Ukraine. He is the Fellow SPIE member and EuMA member. He is authored over 500 scientific publications and conference papers, 8 books, and more than 30 patents. The area of his scientific interests includes physics of semiconductors, low-dimensional systems, IR and THz physics. https://orcid.org/0000-0003-0906-0563

Joanna Gumenjuk-Sichevska received her PhD degree (1991) and DrSc degree (2021) from the V. Lashkaryov Institute of Semiconductor Physics, NAS of Ukraine. Currently she is Leading Researcher at the same institute. Her research interests include transport and optical properties of low-dimensional structures, optoelectronics in a field of IR and THz photodetectors. E-mail: gumenjuk@gmail.com, https://orcid.org/0000-0003-1816-9819

Sergey Danilov received the PhD degree from the St.-Petersburg State Polytechnic University in 1999. Since 2002, he has been Research Fellow at the Terahertz Center, University of Regensburg, Germany. His research interests include semiconductor physics, nanoelectronics, phenomena under IR, THz excitation.
E-mail: sergey.danilov@physik.uni-regensburg.de, https://orcid.org/0000-0003-1910-6887

Zinoviia Tsybrii, Leading researcher at the V. Lashkaryov Institute of Semiconductor Physics, NAS of Ukraine. She defended PhD thesis in Physics and Mathematics in 2000 and DrSc dissertation in 2021 at the same institute. She is authored over 150 publications, 3 patents, 4 textbooks. The area of her scientific interests includes physics and technology of semiconductor materials, hetero-structures and devices (IR and THz detectors, nanomaterials, *etc*.).
E-mail: tsybrii@isp.kiev.ua, http://orcid.org/0000-0003-1718-5569

Спін-залежний поляризаційний фотовідгук у HgCdTe болометрах на гарячих електронах

Ф.Ф. Сизов, Ж.В. Гуменюк-Сичевська, С.Н. Данилов, З.Ф. Цибрій

Анотація. У статті повідомляється про виявлення сильних поляризаційно-залежних фотовідгуків у зміщених і незміщених болометрах на гарячих електронах на основі тонких шарів прямозонного вузькощілинного (E_g = 0,084 еВ при T = 80 K) HgCdTe з приймальними антенами у випадку еліптично поляризованого ТГц випромінювання. Вважається, що спостережувані ефекти пов'язані зі спіновим розщепленням Рашби в HgCdTe, викликаним великою спін-орбітальною взаємодією. Досліджувані детектори демонструють залежну від поляризації вільних носіїв чутливість до лазерного випромінювання з $h\nu \approx$ 0,0044 еВ (ν = 1,07 ТГц) та 0,0025 еВ (ν = 0,6 ТГц), тобто з енергіями фотонів, які набагато менші за ширину забороненої зони ($h\nu << E_g$) при T = 80 і 300 K. Показано, що поляризаційно-залежний фотострум у HgCdTe болометрах на гарячих електронах з прикладеним зовнішнім постійним електричним полем (зміщені фоторезистори) і без нього (незміщені фоторезистори) має кутову залежність зі зміною напрямку при перемиканні спіральності фотона.

Ключові слова: ТГц болометр на гарячих електронах, зв'язаний з антеною, ТГц еліптично поляризоване випромінювання, залежний від поляризації фотовідгук, вузькощілинний HgCdTe.